Report

Current Biology

A dicentric bacterial chromosome requires XerC/D site-specific recombinases for resolution

Graphical abstract

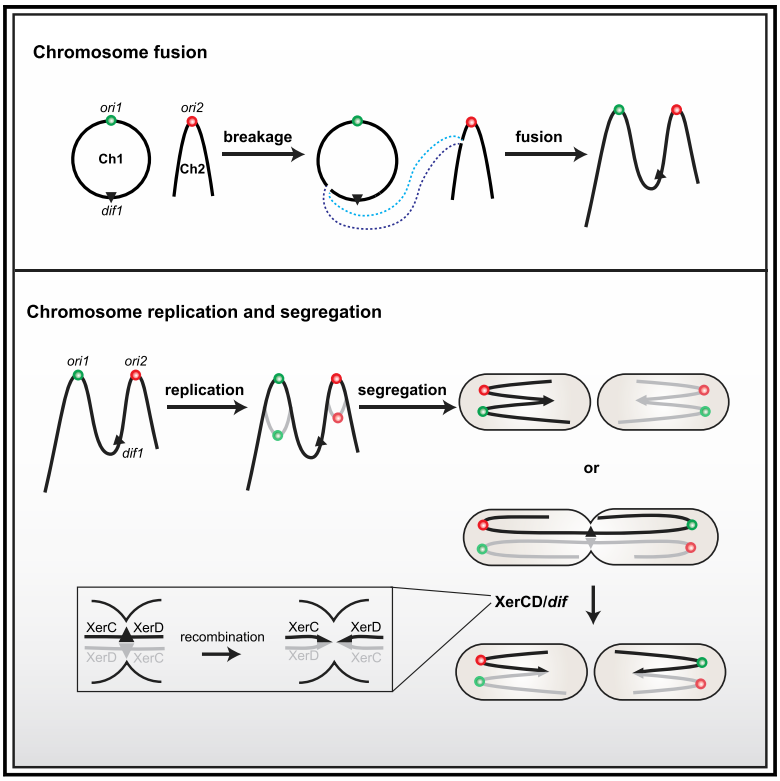

Highlights

- A commonly used *A. tumefaciens* C58 strain has a linear dicentric chromosome
- The fused chromosome resulted from integration of the circular Ch1 into linear Ch2
- The two replication origins are active and their partitioning systems are essential
- Recombinases XerC/D are essential to resolve this dicentric chromosome

Authors

Qin Liao, Zhongqing Ren, Emma E. Wiesler, Clay Fuqua, Xindan Wang

Correspondence

xindan@indiana.edu

In brief

Bacterial chromosomes usually contain a single replication origin. Liao et al. identify a dicentric, linear bacterial chromosome that contains two active replication origins and their independent partitioning systems. This study reveals that XerC/D site-specific recombinases are required to enable this dramatic shift in genomic architecture.

Liao et al., 2022, Current Biology *32*, 1–10
August 22, 2022
https://doi.org/10.1016/j.cub.2022.06.050

CellPress

Please cite this article in press as: Liao et al., A dicentric bacterial chromosome requires XerC/D site-specific recombinases for resolution, Current Biology (2022), https://doi.org/10.1016/j.cub.2022.06.050

Current Biology

CellPress

Report

A dicentric bacterial chromosome requires XerC/D site-specific recombinases for resolution

Qin Liao,[1,2] Zhongqing Ren,[1,2] Emma E. Wiesler,[1] Clay Fuqua,[1] and Xindan Wang[1,3,*]
[1]Department of Biology, Indiana University, 1001 E 3rd Street, Bloomington, IN 47405, USA
[2]These authors contributed equally
[3]Lead contact
*Correspondence: xindan@indiana.edu
https://doi.org/10.1016/j.cub.2022.06.050

SUMMARY

Unlike eukaryotes and archaea, which have multiple replication origins on their chromosomes, bacterial chromosomes usually contain a single replication origin.[1] Here, we discovered a dicentric bacterial chromosome with two replication origins, which has resulted from the fusion of the circular and linear chromosomes in *Agrobacterium tumefaciens*. The fused chromosome is well tolerated, stably maintained, and retains similar subcellular organization and genome-wide DNA interactions found for the bipartite chromosomes. Strikingly, the two replication origins and their partitioning systems are both functional and necessary for cell survival. Finally, we discovered that the site-specific recombinases XerC and XerD[2] are essential in cells harboring the fused chromosome but not in cells with bipartite chromosomes. Analysis of actively dividing cells suggests a model in which XerC/D are required to recombine the sister fusion chromosomes when the two centromeres on the same chromosome are segregated to opposite cell poles. Thus, faithful segregation of dicentric chromosomes in bacteria can occur because of site-specific recombination between the sister chromatids during chromosome partitioning. Our study provides a natural comparative platform to examine a bacterial chromosome with multiple origins and a possible explanation for the fundamental difference in bacterial genome architecture relative to eukaryotes and archaea.[1]

RESULTS AND DISCUSSION

A. tumefaciens C58 contains a circular chromosome (Ch1), a linear chromosome (Ch2), and two large plasmids (pAtC58 and pTiC58), and has been used as a model to study multipartite genome organization.[3–7] Using genome-wide chromosome conformation capture (Hi-C) assays and fluorescence microscopy, recent studies showed that in the C58 wild-type (WT) strain, the origins of all the four replicons are clustered at the cell pole, and each chromosome has the two replication arms juxtaposed from origin to terminus[6,7] (Figure 1A). However, when we performed Hi-C on a different laboratory lineage of C58, the Hi-C interaction map showed discontinuities (Figure 1B), indicating a genome rearrangement in this particular genetic isolate.

The sequence information garnered in Hi-C prompted us to literally dissect the map and rearrange the pieces to obtain a confluent pattern (Figure S1A). Indeed, we achieved a map with a connected primary diagonal and a continuous secondary diagonal, revealing a putative 4.9 Mb linear chromosome containing both Ch1 and Ch2. We analyzed the Hi-C map and identified the breakpoints to be ~1,790 kb on Ch1 and ~710 kb on Ch2 on NCBI Reference Sequence GCA_000092025.1 (Figure 1B, top). We hypothesized that Ch1 and Ch2 were recombined at these two breakpoints, generating a fused linear chromosome. For simplicity, we refer to this strain as the "fusion strain" as opposed to the WT "original strain" with bipartite chromosomes. We note that the fusion strain also contains a previously described 194-kb deletion from the plasmid pAt (from 206.308 kb to 400.732 kb)[8] and an ~10-kb deletion on Ch1 (from 1,175.9 kb to 1,186.2 kb), which appears to contain cryptic phage genes with no obvious relevance to chromosome topology.

To test the hypothesis of a fused chromosome, we used three approaches. First, we re-arranged the reference sequence and remapped our Hi-C reads. This regenerated the map seen in the "solved puzzle" (Figures 1C and S1A). Second, we performed marker frequency analysis (MFA) of the fusion strain by whole-genome sequencing. When mapped to the original reference genome, the fusion strain showed a disconnected profile with interruptions in slopes (Figure 1B, bottom). When mapped to the rearranged reference genome, MFA plot showed a continuous and smooth curve (Figure 1C, bottom). Finally, we checked the continuity of the DNA molecules using PCR. We designed two pairs of PCR primers flanking the breakpoints (Figure 1D). When amplified from the original strain, 3.1 kb and 3.2 kb PCR products were obtained using F1+R1 and F2+R2, respectively, but no product using F1+R2 or F2+R1. However, the fusion strain gave a reverse pattern (Figure 1F). Altogether, our results show that the fusion strain contains a single large linear chromosome with two replication origins.

To narrow down the fusion site, we compared DNA sequences at the two breakpoints and found two highly similar 1.5 kb regions at 1,793 kb on Ch1 (*Atu1813-Atu1814*) and 713 kb on

Please cite this article in press as: Liao et al., A dicentric bacterial chromosome requires XerC/D site-specific recombinases for resolution, Current Biology (2022), https://doi.org/10.1016/j.cub.2022.06.050

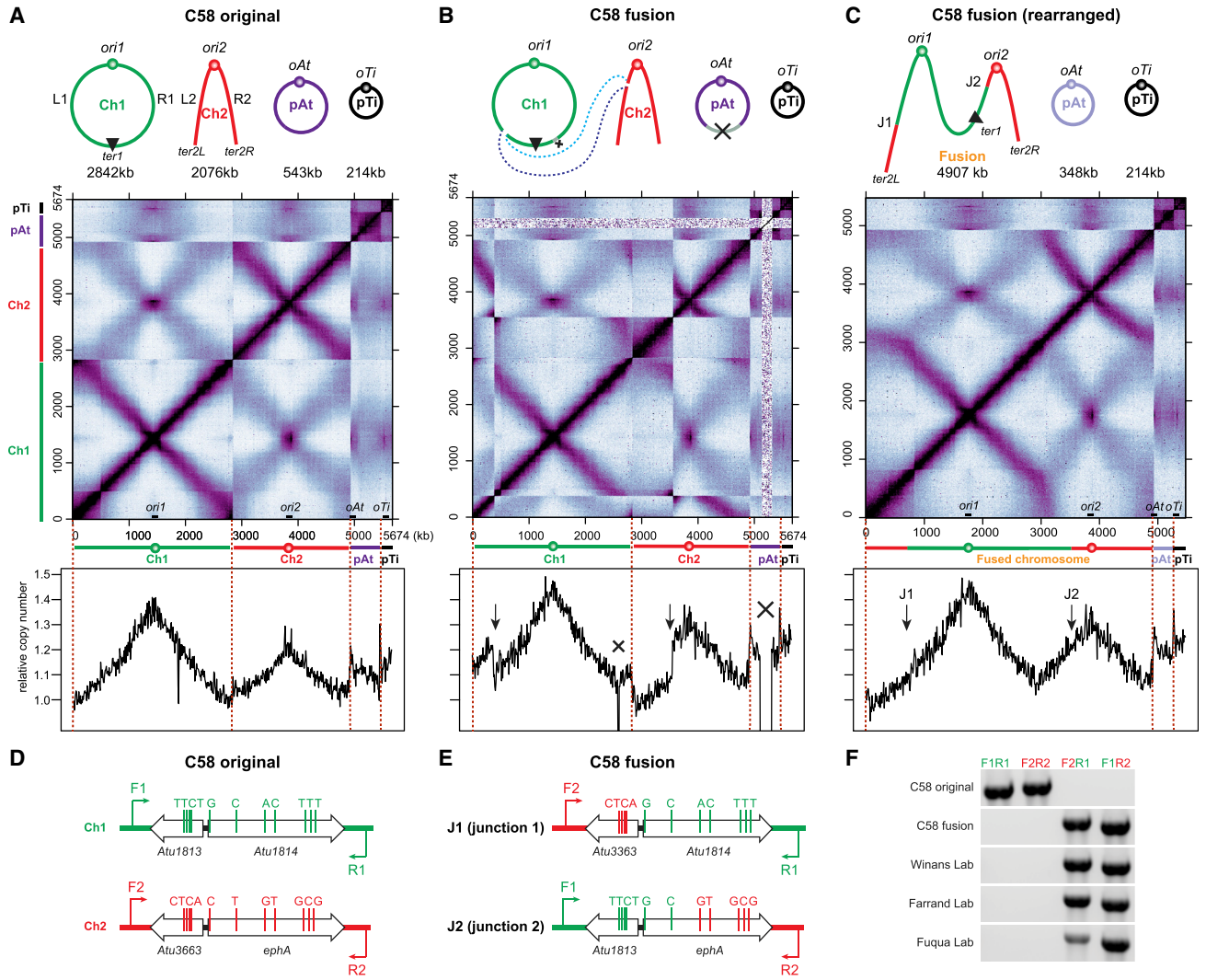

Figure 1. A commonly used wild-type strain of *A. tumefaciens* has the two chromosomes fused into one large linear chromosome

(A–C) Top: schematic diagrams of the replicons in *A. tumefaciens* C58 original strain (A) and the fusion strain (B and C). The original strain contains a circular chromosome (Ch1), a linear chromosome (Ch2), and two plasmids (pAt and pTi). The fusion strain harbors a linear chromosome resulting from the fusion of Ch1 and Ch2, pAt with a deletion, and pTi. Middle: normalized Hi-C contact maps of exponentially growing *A. tumefaciens* C58 original strain (A)[6] and fusion strain (B and C). Hi-C map displays contact frequencies for pairs of 10-kb bins across the genome. In (A) and (B), Hi-C data were mapped to the original C58 reference genome, in which *ori1* was placed at the center of Ch1. In (C), Hi-C data from (B) were mapped to the rearranged reference genome in which deletions were removed. x axis and y axis indicate genomic coordinates. The ends of each replicon are indicated by dark red dotted lines. Bottom: marker frequency analysis (MFA) of exponentially growing original strain (A)[6] and fusion strain (B and C). y axis indicates relative copy number normalized to the copy number of *ter1* (A) or *ter2L* (B and C).

(D) Schematic diagrams depicting regions on Ch1 (green) and Ch2 (red) in the original strain. SNPs are shown as green or red bars. F1/R1 and F2/R2 indicate primer pairs to amplify these regions.

(E) Schematic diagrams depicting fusion junctions on the fused chromosome. Primer pairs of F2/R1 and F1/R2 were used to amplify junction1 (top) and juction2 (bottom), respectively.

(F) Gel electrophoresis analysis of fusion junctions of multiple "wild-type" *A. tumefaciens* C58 strains from different sources.

See also Figure S1.

Ch2 (*Atu3663-ephA*) (Figure 1D) that only differ by 11 SNPs. The high degree of similarity perhaps explains why this rearrangement was not detected in previous whole-genome-sequencing experiments.[8] Comparison of the Sanger sequencing results of the PCR products indicated a strand exchange between *Atu1814* and *ephA* within the first ~300 bp (Figures 1E and 1F). It is likely that a double-stranded break happened at *ephA*, and the highly similar sequence on *Atu1814* provided the repair template for homologous recombination; this single crossover event may have led to the fusion of the two chromosomes.

To test whether the fusion strain is commonly used in the *Agrobacterium* research community, we analyzed over 20 of C58 WT strains or direct derivatives from 16 labs using PCR and Hi-C. To our surprise, WT stocks from 7 labs contain the

Please cite this article in press as: Liao et al., A dicentric bacterial chromosome requires XerC/D site-specific recombinases for resolution, Current Biology (2022), https://doi.org/10.1016/j.cub.2022.06.050

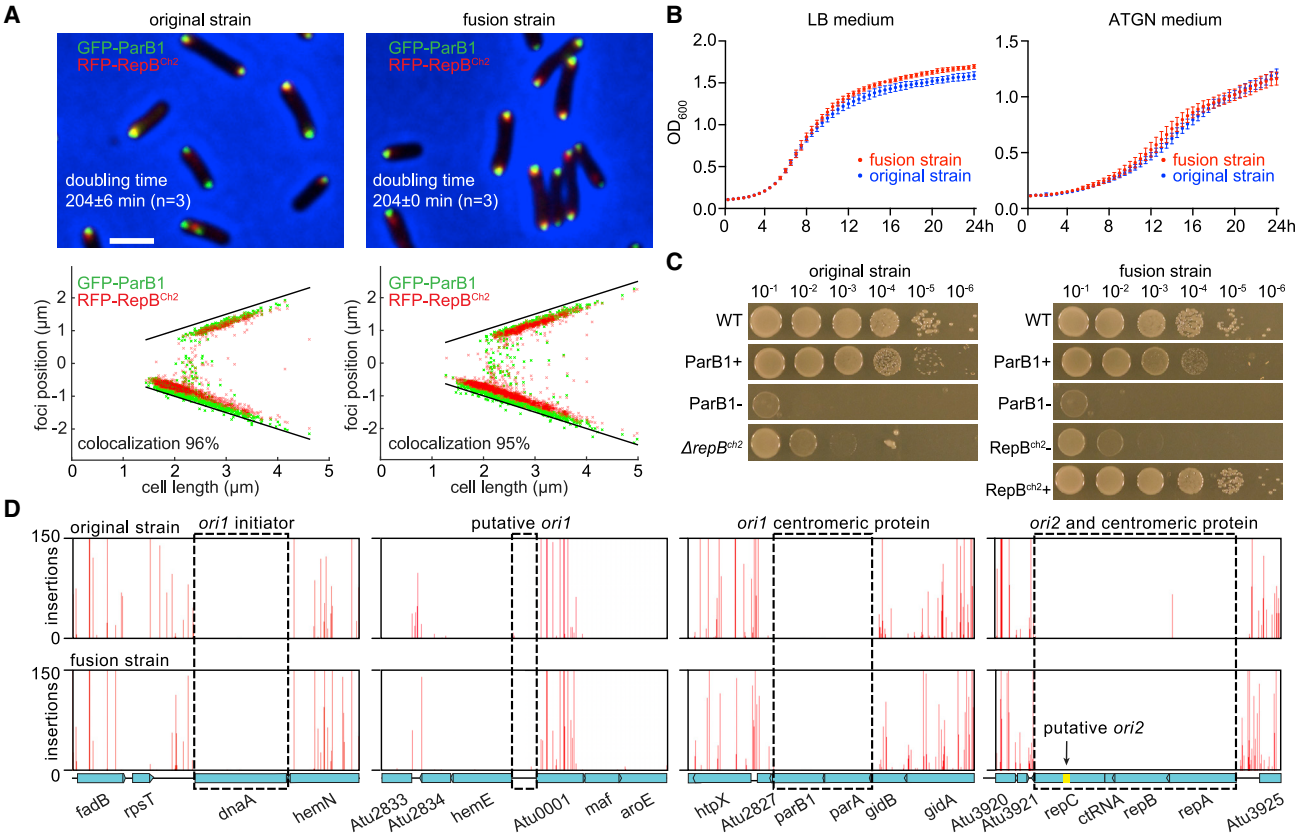

Figure 2. The fusion and original strains exhibit similar characteristics for growth, chromosome localization, replication, and partition

(A) Localization of *ori1* and *ori2* in the original strain (AtWX263) and the fusion strain (AtWX366). The replication origins were visualized by expressing GFP-ParB1 (green, *ori1*) and RFP-RepB^{Ch2} (red, *ori2*) from a pSRKKm-based plasmid. Top: fluorescence images. Scale bar represents 2 μm. The doubling time of these cells growing in ATGN medium was indicated. Bottom: plots showing relative position of foci. Black lines indicate positions of two cell poles.

(B) Growth curves of the WT original and WT fusion strains growing in LB broth (left) or ATGN medium (right) in a microplate at 30°C on a plate reader with shaking. Optical density at 600 nm was measured at an interval of 30 min. The error bars indicate the SD of six biological replicates combined from two independent experiments.

(C) Ten-fold serial dilutions of indicated strains were spotted on LB plates. ParB1 depletion strains (AtWX192 and AtWX194) have the endogenous *parB1* gene deleted and an ectopic copy of *parB1* expressed from *Ptral-riboswitch* at the *tetRA* locus.[6] 1 μM AHL and 2 mM theophylline were added into ParB1+ plates. Although the cells were extremely sick, *repB^{Ch2}* was successfully deleted from the original strain (Δ*repB^{Ch2}*, AtWX089) but not from the fusion strain. To deplete RepB^{Ch2} from the fusion strain (AtWX025), the endogenous *repB^{ch2}* was deleted and an ectopic copy of *repB^{ch2}* was expressed from *Plac* at the T7 attachment site. 0.5 mM IPTG was added into RepB^{Ch2} + plates.

(D) Tn-seq plots showing transposon intolerance in the two replication origins and two centromeres in WT original strain (top) and WT fusion strain (bottom). y axis indicates the number of sequencing reads at each insertion site. x axis indicates gene locus. Black dotted rectangles highlight regions of interest. This screen was carried out in LB medium. Similar results were observed when cells were grown in minimal ATGN medium (Figure S1B).

See also Figure S1.

fused chromosome[5,8–11] (Figure 1F; Table S1). It is likely that this fusion strain is even more widely dispersed than revealed through this limited analysis. By tracing the historical distribution of these strains, we suspect that this fusion event happened while the strain was propagated by the laboratory of Stephen K. Farrand. Then the fusion strain was distributed to other labs.

Despite the fact that the two chromosomes were fused into a single DNA molecule, the replication "arms" on either side of each origin interacted along their length and the origins of all the replicons remained clustered (Figures 1A and 1C). Fluorescence images and detailed analysis showed that the localization of the two origins was very similar between the original and the fusion strains (Figure 2A). In shaken liquid cultures, these two strains had near-identical doubling times (~204 min in defined ATGN medium and ~90 min in nutrient-rich LB medium) and very similar growth curves, although the fusion strain showed a marginal but reproducible growth advantage (Figure 2B), which is consistent with growth competition assays published previously.[8] Thus, the fused chromosome was well tolerated by the cell, behaved similarly to the bipartite chromosomes in terms of localization and genome-wide organization, and did not pose an obvious growth difference, although subtle growth differences dependent on environmental conditions are possible. We note that the fusion strain is fully virulent,[12,13] even though the level of virulence was not directly compared with the original strain.

Bacterial chromosomes typically contain a single replication origin and one centromere. However, our MFA plots indicated

Please cite this article in press as: Liao et al., A dicentric bacterial chromosome requires XerC/D site-specific recombinases for resolution, Current Biology (2022), https://doi.org/10.1016/j.cub.2022.06.050

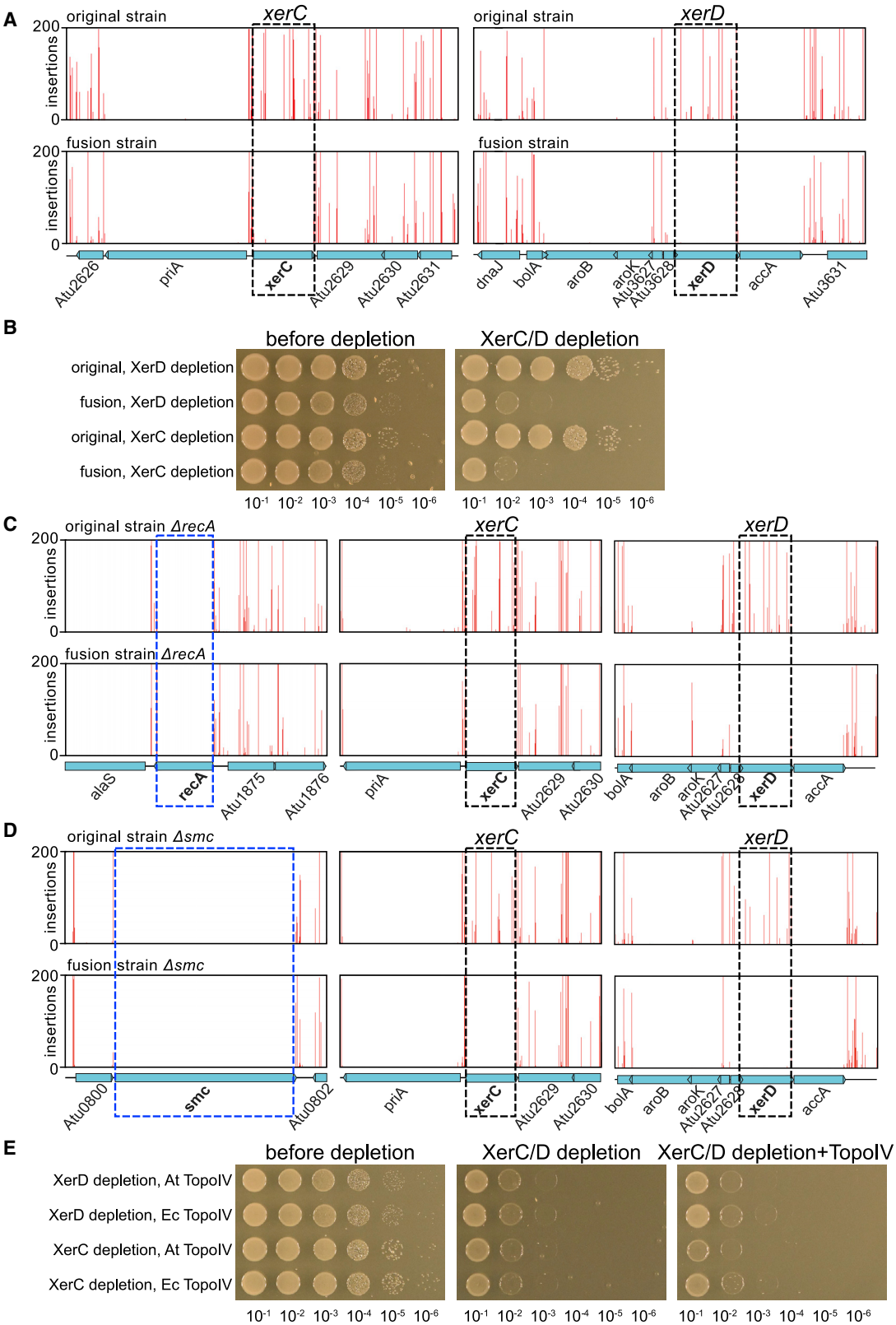

(legend on next page)

Please cite this article in press as: Liao et al., A dicentric bacterial chromosome requires XerC/D site-specific recombinases for resolution, Current Biology (2022), https://doi.org/10.1016/j.cub.2022.06.050

that both origins on the fused chromosome were functional and fired at levels similar to the original strain;[6] the pair of replication forks tracking from the same origin progressed at the similar speed as indicated by the slope on the curve (Figures 1A and 1C). We next questioned whether both origins are necessary for cell survival. We performed transposon mutagenesis coupled to sequencing (Tn-seq) to identify all essential genes in the original and fusion strains. Mutant libraries were constructed by introducing a *mariner* transposon into both strains. Approximately 1×10^6 mutants derived from each strain were harvested and processed for next-generation sequencing. In both strains, no transposon insertion was detected at the replication origins (*ori1* and *ori2*), the replication initiators (*dnaA* for *ori1* and *repC* for *ori2*), or the centromeric or partitioning factors (*parAB* for *ori1* and *repAB* for *ori2*), regardless of growth media (Figures 2D and S1B). Consistent with the Tn-seq results, we were unable to delete the genes encoding the centromeric proteins, ParB1 or $RepB^{Ch2}$, from the fused chromosome. Instead, the endogenous deletions were successful only in depletion strains in which we expressed an ectopic copy: Figure 2C shows that in the absence of ParB1 or $RepB^{Ch2}$ the fusion strain was as debilitated as the original strain. These results indicate that replication origins and centromeres of both *ori1* and *ori2* are required for the viability of the fusion strain. This surprising finding is being investigated further in a separate study.

For the original strain, our Tn-seq experiments identified all the essential genes reported previously.[14] We next investigated whether genes that were not essential in the original strain had become essential in the fusion strain. In Tn-seq, *xerC* and *xerD* [2] were the only two genes that had dramatically decreased insertions in the fusion strain compared with the original strain. Similar results were obtained using either LB or ATGN medium (Figures 3A and S2A). To validate the Tn-seq results, we sought to delete *xerC* and *xerD*. As expected, we successfully deleted these genes in the original strain (Figure S2E) but not in the fusion strain. Therefore, we generated *xerC* and *xerD* depletion strains in which the endogenous promotors of these two genes were disrupted by inserting an IPTG-inducible promoter combined with a theophylline-inducible riboswitch (*Plac-riboswitch*).[15,16] We found that the fusion strain was not able to form colonies when *xerC* or *xerD* was depleted, while the original strains grew similarly with or without inducers (Figures 3B and S2B). Thus, *xerC* and *xerD* are required for the survival of the fusion strain but not of the original strain. Given that the fusion strain has a 10-kb deletion on Ch1 and a 194-kb deletion on pAt, we queried whether *xerC/D* has a synthetic lethal relationship with any of the missing genes. We performed Tn-seq on a Δ*xerD* original strain and found that the genes that were missing in the fusion strain tolerated transposon insertions (Figure S3). Thus, *xerC/D*'s essentiality in the fusion strain is not due to these missing genes.

The *xerC* and *xerD* gene products are broadly conserved site-specific recombinases, which act on a 28-bp *dif* site at the terminus region of circular bacterial chromosomes to resolve chromosome dimers.[2,17–23] This recombination is activated by the very C-terminal (gamma) domain of FtsK, FtsKγ, which is directed by the FtsK-orienting polar sequences (KOPS) to translocate to the *dif* site.[24–27] Although the N-terminal domain of FtsK is essential, it is common that *xerC*, *xerD*, and *ftsKγ* are non-essential.[24,25] To understand why *xerC* and *xerD* became essential in the fusion strain, we first experimentally determined the binding sites of XerC and XerD in *A. tumefaciens*. We tagged endogenous copies of XerC and XerD with GFP and performed chromatin immunoprecipitation sequencing (ChIP-seq) using anti-GFP antibodies. ChIP-seq analysis indicated that in both the fusion and original strains, XerC-GFP and XerD-GFP had two enrichment peaks, one on Ch1 and one on pAt (Figure S2C). Using the MEME suite (http://meme-suite.org/) for motif search, we identified *dif1* on Ch1 and dif^{pAt} on pAt (Figure S2D). To test the essentiality of these *dif* sites, we successfully deleted both *dif* sites from the original strain and dif^{pAt} from the fusion strain (Figure S2E), but we were not able to delete *dif1* from the fusion strain. Consistent with this, our Tn-seq results showed that only *dif1* in the fusion strain did not tolerate transposon insertions (Figure S2F). Finally, although *ftsK* was indicated as essential for both strains in Tn-seq, a closer examination revealed that *ftsKγ* tolerated transposon insertions in the original strain but not in the fusion strain (Figure S2G). Altogether, these results indicate that XerC/D recombination at *dif1* activated by FtsKγ is essential for the survival of the fusion strain. We note that *dif1* is still at the convergence of KOPS in the fusion strain, indicating proper function of this system (Figure S2H).

Based on the established functions of XerC/D recombinases in resolving chromosome dimers generated by homologous recombination in RecA+ strains,[28] unloading of structural maintenance of chromosome (SMC) complexes from the replication terminus,[29] and decatenating the intertwined sister chromosomes in a stepwise manner,[30–32] we tested whether the essentiality of XerC/D for the fused chromosome could be suppressed by *ΔrecA*, *Δsmc*, or increasing decatenation activity by overexpressing topoisomerase IV (Topo IV). We performed Tn-seq in *ΔrecA* or *Δsmc* in the backgrounds of both original and fusion

Figure 3. XerC and XerD are required for the survival of the fusion strain

(A) Tn-seq plots showing transposon insertions at *xerC/xerD* loci and flanking regions in the WT original (top) and WT fusion (bottom) strains. *xerC* and *xerD* genes tolerated insertions in the original strain but not in the fusion strain. This screen was performed in LB. Similar results were observed for ATGN medium (Figure S2A).

(B) Validation of essentiality of *xerD* and *xerC* using depletion constructs (AtWX323, AtWX327, AtWX331, and AtWX332). Ten-fold serial dilutions of indicated strains were spotted on LB plates. The depletion constructs had the promotor of *xerD* or *xerC* replaced by *Plac-riboswitch*. 2 mM theophylline and 0.5 mM IPTG were added as inducers. Similar results were observed for ATGN medium (Figure S2B).

(C) Tn-seq performed in *ΔrecA* original strain (AtWX398, top) and Δ*recA* fusion strain (AtWX387, bottom).

(D) Tn-seq performed in *Δsmc* original strain (AtWX108, top) and Δ*smc* fusion strain (AtWX035, bottom).

(E) Ten-fold serial dilutions of indicated strains were spotted on LB plates. XerC/D depletion strains contain cumate-inducible plasmids expressing *A. tumefaciens* Topo IV (AtWX502 and AtWX503) or *E. coli* Topo IV (AtWX540 and AtWX541). 300 μg/mL of kanamycin were applied on all plates for plasmid maintenance. The following inducers were added: 0.5 mM IPTG (left), none (middle), 2 mM cumate (right).

See also Figures S2 and S3.

Please cite this article in press as: Liao et al., A dicentric bacterial chromosome requires XerC/D site-specific recombinases for resolution, Current Biology (2022), https://doi.org/10.1016/j.cub.2022.06.050

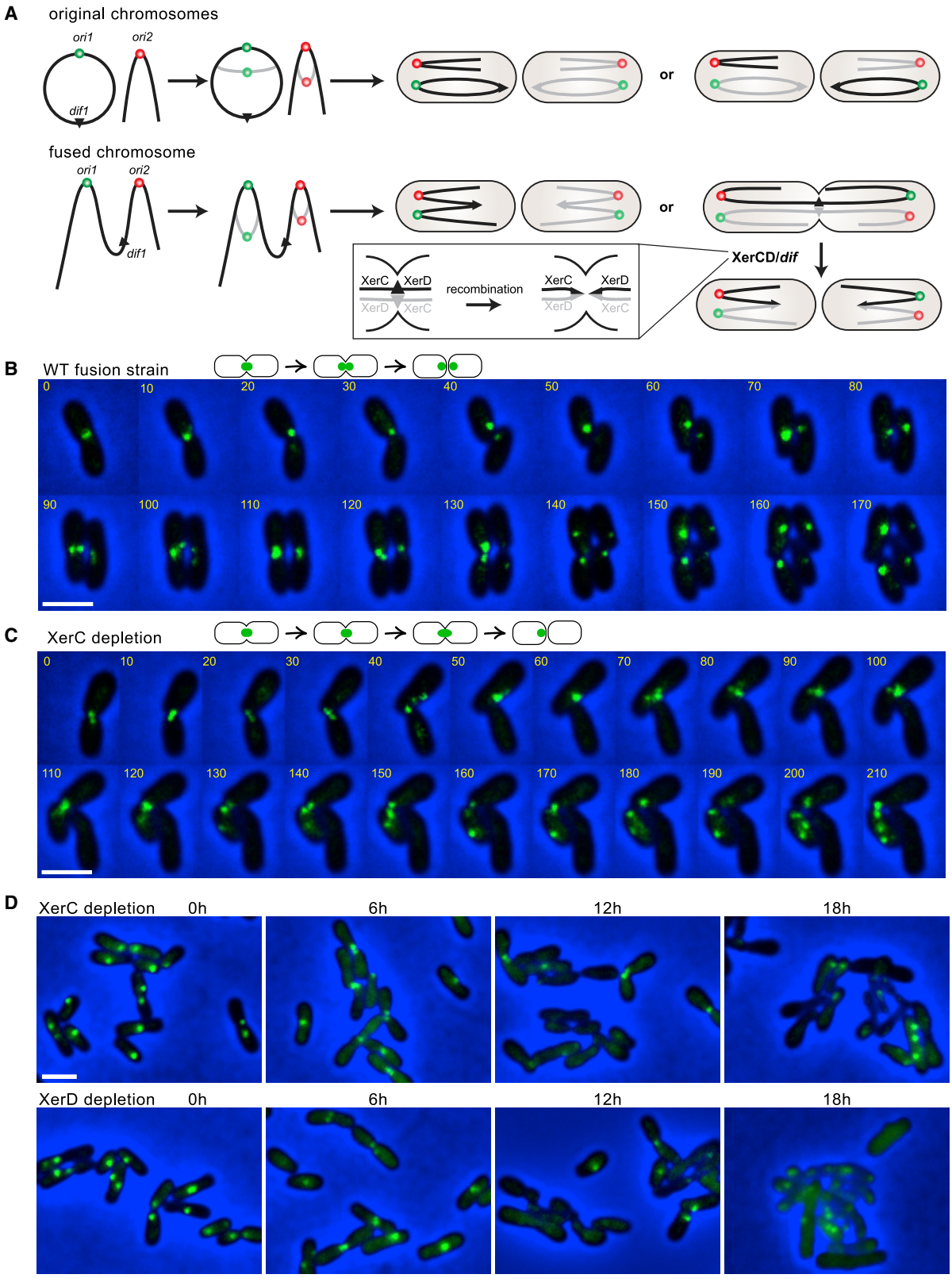

(legend on next page)

Please cite this article in press as: Liao et al., A dicentric bacterial chromosome requires XerC/D site-specific recombinases for resolution, Current Biology (2022), https://doi.org/10.1016/j.cub.2022.06.050

strains and found that *xerC* and *xerD* were still essential in the mutated fusion strains (Figures 3C and 3D). Furthermore, overexpression of *A. tumefaciens* Topo IV or *E. coli* Topo IV was unable to rescue the growth defect of XerC/D depletion strains (Figure 3E). Thus, the essentiality of XerC/D is not related to RecA-dependent recombination, the presence of SMC, or insufficient decatenation of the fused chromosome.

Thus, we hypothesized that the essentiality of XerC/D is due to the topology of the fused chromosome: if the segregation of the origins is random, for every cell generation, in 50% of cells, the two origins on the same chromosome will migrate to opposite poles, resulting in segregation problems, breakage of DNA, and potentially cell death unless resolved by the XerC/D/*dif1* system (Figure 4A). To directly observe the effect of XerC and XerD depletion on *dif1* segregation in the fusion strain, we visualized the *dif1* locus and tracked the progress of its segregation in time-lapse microscopy. In the WT fusion strain, cells were born with a single *dif1* focus localized and remained at the new cell pole as the cell grew. The *dif1* focus then moved to the midcell and split into two foci before cell division (Figure 4B). When XerC was depleted, the majority of cells started with a single *dif1* focus remaining at the deeply constricted septum. Then the cells did not seem to completely divide; the daughter cells were still connected to each other, forming a cluster of branched cells with randomly distributed *dif1* foci (Figure 4C). For comparison, we simultaneously labeled the end of the linear chromosome by inserting an *mcherry-parB*^{P1}*-parS*^{P1} visualization cassette at 39.8 kb from right terminus of the fused chromosome (*ter2R*). When XerC was depleted, unlike *dif1*, *ter2R* was replicated and segregated into two daughter cells normally (Figure S4A). Thus, XerC depletion impaired cell division and *dif1* segregation but not *ter2R* segregation.

For quantitative measurement, we analyzed a large number of cells in a time course experiment during XerC or XerD depletion (Figure S4B). In the WT fusion strain during exponential growth, 67.7% of cells contained a single *dif1* focus at the cell pole or the midcell, 4.8% of cells had two foci before constriction, and 20.5% of cells contained two foci and a constricting septum. In XerC or XerD depletion strain, prior to depletion, the *dif1* locus behaved similarly to that in WT fusion strain. However, within the 6 h depletion of XerC or XerD, we observed a roughly 2-fold increase in the number of deeply constricted cells with one or two *dif1* foci. After 12 h of depletion, the percentage of deeply constricted cells remained while the number of cells without foci increased over 3-fold compared with the 6 h time point. After 18 h of depletion, the majority of cells did not contain a *dif1* focus and cells exhibited branchy and other abnormalities in cell shape. Our time-lapse and snapshot imaging experiments are consistent with the idea that XerC/D are required to resolve the *dif1* region of the fused chromosome. The depletion of XerC/D led to the delayed segregation of *dif1* site, blocked cell division, frequent guillotining of DNA at the septum, and cell death.

Here, we discovered a linear dicentric chromosome that has resulted from the fusion of a circular and a linear chromosome in the multipartite genome of *A. tumefaciens*. We showed that this fusion event did not confer to the cell dramatic growth advantages or disadvantages and the dicentric chromosome exhibited cellular localization and the features of genome-wide organization resembling those observed for the original strain. Moreover, both replication origins on this fused chromosome retained independent replication and segregation programs. We found that this fusion strain is stably maintained and has been commonly used in the research community (Table S1). Although non-engineered chromosome fusions have been reported in several bacterial species,[33–38] they frequently lead to slower growth, are unstable, and can be reversed. It is thus surprising that the fusion strain discussed here can cope so effectively with its complex genome structure. Our genetic screen revealed that the fusion strain requires the XerC/D/*dif1* system for proper chromosome segregation and cell division, which is likely a consequence of the independent origin segregation.

Roughly 10% of sequenced bacteria, most of which are pathogens or symbionts, have multipartite genomes.[39] It has been proposed that the secondary chromosomes have evolved from plasmids acquiring essential genes.[40] Multipartite genomes allow more rapid genome duplication, which is advantageous for those species. However, compared with a single chromosome, a split genome is more complicated to maintain and requires coordination between replicons during replication and segregation. Why would bacteria not evolve multiple replication origins on a single chromosome to confer a faster genome duplication rate and simplify the management of multiple replicons, analogous to eukaryotes and many archaea? Our discovery here suggests that the concurrent DNA replication and segregation in bacteria can be incompatible with multiple replication origins or centromeres on the same chromosome, if it is not co-evolved with an XerC/D/*dif*-like system between each of the multiple origins, and/or properly oriented KOPS for FtsK to pump the DNA into the correct daughter cell.

The segregation of a bacterial chromosome is driven by partitioning proteins that bind to the centromere region of each chromosomal copy and drag them to opposite cell poles.[41] In a multipartite genome, faithful segregation of each replicon relies

Figure 4. XerC and XerD are required to segregate the fused chromosome

(A) Schematic model. After the initiation of replication, two copies of *ori1* and *ori2* independently move into opposite daughter cells. In the original strain (top), either combination leads to viable cells. In the fusion strain (bottom), the cells will survive when *ori1* and *ori2* on the same DNA molecule are distributed in the same cell half. However, when they are positioned in opposite cell halves, cell division is blocked until the sister fusion chromosomes are recombined by XerC/D at *dif1*.

(B and C) Time-lapse progression of *dif1* dynamics during the cell cycle in WT fusion (AtWX455) (B) and XerC-depleted fusion strain (AtWX467) (C) growing on LB agarose pad. *dif1* was visualized by inserting the visualization cassette, *ygfp-parB*^{pMT1}*-parS*^{pMT1}, at the position ~22 kb away from *dif1*. For (C), XerC was pre-depleted in liquid LB medium without inducers for 6 h before the start of time-lapse microscopy. The time interval was 10 min. Scale bar represents 2 μm.

(D) Localization of *dif1* in time course of XerC depletion (AtWX467, top) and XerD depletion (AtWX471, bottom) in the fusion strain. Cells were grown in LB medium with the addition of 0.5 mM IPTG and 2 mM theophylline, collected and resuspended in medium without inducers to start depletion. The quantitative analysis can be found in Figure S4B.

See also Figure S4.

on their own partitioning systems.[6,42] The dicentric chromosome we discovered here generates a segregation problem that a multipartite genome avoids: independent segregation of the origins that translocate different parts of the same chromosome into opposite cell poles (Figure 4A). In contrast, eukaryotes and many archaea have multiple replication origins but a single centromere for each chromosome. These species employ temporal separation of DNA replication and segregation to ensure genome integrity. The dicentric bacterial chromosome we discovered here has survived and flourished, but this might be a serendipitous situation in which the XerC/D/*dif* system happens to be at the appropriate location to correct the opposite localization of each origin. The stable maintenance of this remarkable dicentric chromosome captures a snapshot of genome and species evolution through the survival of an accident and has revealed a possible explanation for the fundamental difference in genome architecture between bacteria and eukaryotes/archaea.

STAR★METHODS

Detailed methods are provided in the online version of this paper and include the following:

- KEY RESOURCES TABLE
- RESOURCE AVAILABILITY
  - Lead contact
  - Materials availability
  - Data and code availability
- EXPERIMENTAL MODEL AND SUBJECT DETAILS
  - Bacterial strains and growth
- METHODS DETAILS
  - Hi-C
  - ChIP-seq
  - Identification of *dif* sites
  - Whole genome sequencing (WGS)
  - Transposon insertion sequencing (Tn-seq)
  - Growth curve measurement
  - Fluorescence microscopy analysis
  - Plasmid construction
  - Strain construction
- QUANTIFICATION AND STATISTICAL ANALYSIS
  - Localization of *ori1* and *ori2*
  - Measurements of doubling time and growth curve
  - Quantitative analysis of *dif1* localization patterns

SUPPLEMENTAL INFORMATION

Supplemental information can be found online at https://doi.org/10.1016/j.cub.2022.06.050.

ACKNOWLEDGMENTS

We thank the Indiana University Center for Genomics and Bioinformatics for assistance with high-throughput sequencing. We thank Ankur Dalia for the transposon plasmid (pTND2823); Julia van Kessel for plate reader; Pam Brown, Patricia Zambryski, and John Zupan for strains and plasmids; and Dan Kearns and David Rudner for reading the manuscript. We thank the entire *Agrobacterium* community for sharing their C58 strains for characterization. Support for this work comes from National Institutes of Health R01GM141242 (X.W.) and R01GM120337 (C.F.).

AUTHOR CONTRIBUTIONS

Q.L., Z.R., and X.W. designed the study; Q.L. and Z.R. constructed plasmids and strains and performed Tn-seq and whole-genome sequencing. Q.L. performed ChIP-seq, microscopy experiments, and analyses. Z.R. and X.W. performed Hi-C experiments and analyses. E.E.W. assisted with strain building. C.F. coordinated strain acquisitions and provided reagents. Q.L. and X.W. wrote the manuscript with input from Z.R. and C.F. X.W. supervised the entire study.

DECLARATION OF INTERESTS

The authors declare no competing interests.

Received: April 13, 2022
Revised: May 24, 2022
Accepted: June 15, 2022
Published: July 6, 2022

REFERENCES

1. Robinson, N.P., and Bell, S.D. (2005). Origins of DNA replication in the three domains of life. FEBS J. *272*, 3757–3766. https://doi.org/10.1111/j.1742-4658.2005.04768.x.
2. Blakely, G., May, G., McCulloch, R., Arciszewska, L.K., Burke, M., Lovett, S.T., and Sherratt, D.J. (1993). Two related recombinases are required for site-specific recombination at dif and cer in E. coli K12. Cell *75*, 351–361. https://doi.org/10.1016/0092-8674(93)80076-q.
3. Kahng, L.S., and Shapiro, L. (2003). Polar localization of replicon origins in the multipartite genomes of Agrobacterium tumefaciens and Sinorhizobium meliloti. J. Bacteriol. *185*, 3384–3391. https://doi.org/10.1128/JB.185.11.3384-3391.2003.
4. Slater, S.C., Goldman, B.S., Goodner, B., Setubal, J.C., Farrand, S.K., Nester, E.W., Burr, T.J., Banta, L., Dickerman, A.W., Paulsen, I., et al. (2009). Genome sequences of three agrobacterium biovars help elucidate the evolution of multichromosome genomes in bacteria. J. Bacteriol. *191*, 2501–2511. https://doi.org/10.1128/JB.01779-08.
5. Robalino-Espinosa, J.S., Zupan, J.R., Chavez-Arroyo, A., and Zambryski, P. (2020). Segregation of four Agrobacterium tumefaciens replicons during polar growth: PopZ and PodJ control segregation of essential replicons. Proc. Natl. Acad. Sci. USA *117*, 26366–26373. https://doi.org/10.1073/pnas.2014371117.
6. Ren, Z., Liao, Q., Karaboja, X., Barton, I.S., Schantz, E.G., Mejia-Santana, A., Fuqua, C., and Wang, X. (2022). Conformation and dynamic interactions of the multipartite genome in Agrobacterium tumefaciens. Proc. Natl. Acad. Sci. USA *119*. e2115854119. https://doi.org/10.1073/pnas.2115854119.
7. Ren, Z., Liao, Q., Barton, I.S., Wiesler, E.E., Fuqua, C., and Wang, X. (2022). Centromere interactions promote the maintenance of the multipartite genome in Agrobacterium tumefaciens. mBio. Published online May 10, 2022. https://doi.org/10.1128/mbio.00508-22.
8. Morton, E.R., Merritt, P.M., Bever, J.D., and Fuqua, C. (2013). Large deletions in the pAtC58 megaplasmid of Agrobacterium tumefaciens can confer reduced carriage cost and increased expression of virulence genes. Genome Biol. Evol. *5*, 1353–1364. https://doi.org/10.1093/gbe/evt095.
9. Figueroa-Cuilan, W., Daniel, J.J., Howell, M., Sulaiman, A., and Brown, P.J.B. (2016). Mini-Tn7 insertion in an artificial attTn7 site enables depletion of the essential master regulator CtrA in the phytopathogen Agrobacterium tumefaciens. Appl. Environ. Microbiol. *82*, 5015–5025. https://doi.org/10.1128/AEM.01392-16.
10. Fuqua, C., Burbea, M., and Winans, S.C. (1995). Activity of the Agrobacterium Ti plasmid conjugal transfer regulator TraR is inhibited by the product of the traM gene. J. Bacteriol. *177*, 1367–1373. https://doi.org/10.1128/jb.177.5.1367-1373.1995.

11. Farrand, S.K., and Dessaux, Y. (1986). Proline biosynthesis encoded by the noc and occ loci of Agrobacterium Ti plasmids. J. Bacteriol. *167*, 732–734. https://doi.org/10.1128/jb.167.2.732-734.1986.

12. Heindl, J.E., Hibbing, M.E., Xu, J., Natarajan, R., Buechlein, A.M., and Fuqua, C. (2015). Discrete responses to limitation for iron and manganese in Agrobacterium tumefaciens: influence on attachment and biofilm formation. J. Bacteriol. *198*, 816–829. https://doi.org/10.1128/JB.00668-15.

13. Hibbing, M.E., and Fuqua, C. (2011). Antiparallel and interlinked control of cellular iron levels by the Irr and RirA regulators of Agrobacterium tumefaciens. J. Bacteriol. *193*, 3461–3472. https://doi.org/10.1128/JB.00317-11.

14. Curtis, P.D., and Brun, Y.V. (2014). Identification of essential alphaproteobacterial genes reveals operational variability in conserved developmental and cell cycle systems. Mol. Microbiol. *93*, 713–735. https://doi.org/10.1111/mmi.12686.

15. Zupan, J.R., Grangeon, R., Robalino-Espinosa, J.S., Garnica, N., and Zambryski, P. (2019). GROWTH POLE RING protein forms a 200-nm-diameter ring structure essential for polar growth and rod shape in Agrobacterium tumefaciens. Proc. Natl. Acad. Sci. USA *116*, 10962–10967. https://doi.org/10.1073/pnas.1905900116.

16. Topp, S., Reynoso, C.M.K., Seeliger, J.C., Goldlust, I.S., Desai, S.K., Murat, D., Shen, A., Puri, A.W., Komeili, A., Bertozzi, C.R., et al. (2010). Synthetic riboswitches that induce gene expression in diverse bacterial species. Appl. Environ. Microbiol. *76*, 7881–7884. https://doi.org/10.1128/AEM.01537-10.

17. Carnoy, C., and Roten, C.A. (2009). The dif/Xer recombination systems in proteobacteria. PLoS One *4*, e6531. https://doi.org/10.1371/journal.pone.0006531.

18. Recchia, G.D., and Sherratt, D.J. (1999). Conservation of xer site-specific recombination genes in bacteria. Mol. Microbiol. *34*, 1146–1148. https://doi.org/10.1046/j.1365-2958.1999.01668.x.

19. Yen, M.R., Lin, N.T., Hung, C.H., Choy, K.T., Weng, S.F., and Tseng, Y.H. (2002). oriC region and replication termination site, dif, of the Xanthomonas campestris pv. campestris 17 chromosome. Appl. Environ. Microbiol. *68*, 2924–2933. https://doi.org/10.1128/AEM.68.6.2924-2933.2002.

20. Val, M.E., Kennedy, S.P., El Karoui, M., Bonné, L., Chevalier, F., and Barre, F.X. (2008). FtsK-dependent dimer resolution on multiple chromosomes in the pathogen Vibrio cholerae. PLoS Genet. *4*, e1000201. https://doi.org/10.1371/journal.pgen.1000201.

21. Sciochetti, S.A., Piggot, P.J., and Blakely, G.W. (2001). Identification and characterization of the dif Site from Bacillus subtilis. J. Bacteriol. *183*, 1058–1068. https://doi.org/10.1128/JB.183.3.1058-1068.2001.

22. Neilson, L., Blakely, G., and Sherratt, D.J. (1999). Site-specific recombination at dif by Haemophilus influenzae XerC. Mol. Microbiol. *31*, 915–926. https://doi.org/10.1046/j.1365-2958.1999.01231.x.

23. Nunes-Duby, S.E., Kwon, H.J., Tirumalai, R.S., Ellenberger, T., and Landy, A. (1998). Similarities and differences among 105 members of the Int family of site-specific recombinases. Nucleic Acids Res. *26*, 391–406. https://doi.org/10.1093/nar/26.2.391.

24. Crozat, E., and Grainge, I. (2010). FtsK DNA translocase: the fast motor that knows where it's going. Chembiochem *11*, 2232–2243. https://doi.org/10.1002/cbic.201000347.

25. Grainge, I. (2013). Simple topology: FtsK-directed recombination at the dif site. Biochem. Soc. Trans. *41*, 595–600. https://doi.org/10.1042/BST20120299.

26. Sivanathan, V., Allen, M.D., de Bekker, C., Baker, R., Arciszewska, L.K., Freund, S.M., Bycroft, M., Löwe, J., and Sherratt, D.J. (2006). The FtsK gamma domain directs oriented DNA translocation by interacting with KOPS. Nat. Struct. Mol. Biol. *13*, 965–972. https://doi.org/10.1038/nsmb1158.

27. Bigot, S., Saleh, O.A., Cornet, F., Allemand, J.F., and Barre, F.X. (2006). Oriented loading of FtsK on KOPS. Nat. Struct. Mol. Biol. *13*, 1026–1028. https://doi.org/10.1038/nsmb1159.

28. Blakely, G., Colloms, S., May, G., Burke, M., and Sherratt, D. (1991). Escherichia coli XerC recombinase is required for chromosomal segregation at cell division. New Biol. *3*, 789–798.

29. Karaboja, X., Ren, Z., Brandão, H.B., Paul, P., Rudner, D.Z., and Wang, X. (2021). XerD unloads bacterial SMC complexes at the replication terminus. Mol. Cell *81*, 756–766.e8. https://doi.org/10.1016/j.molcel.2020.12.027.

30. Ip, S.C., Bregu, M., Barre, F.X., and Sherratt, D.J. (2003). Decatenation of DNA circles by FtsK-dependent Xer site-specific recombination. EMBO J. *22*, 6399–6407. https://doi.org/10.1093/emboj/cdg589.

31. Grainge, I., Bregu, M., Vazquez, M., Sivanathan, V., Ip, S.C.Y., and Sherratt, D.J. (2007). Unlinking chromosome catenanes in vivo by site-specific recombination. EMBO J. *26*, 4228–4238. https://doi.org/10.1038/sj.emboj.7601849.

32. Shimokawa, K., Ishihara, K., Grainge, I., Sherratt, D.J., and Vazquez, M. (2013). FtsK-dependent XerCD-dif recombination unlinks replication catenanes in a stepwise manner. Proc. Natl. Acad. Sci. USA *110*, 20906–20911. https://doi.org/10.1073/pnas.1308450110.

33. Guo, X., Flores, M., Mavingui, P., Fuentes, S.I., Hernández, G., Dávila, G., and Palacios, R. (2003). Natural genomic design in Sinorhizobium meliloti: novel genomic architectures. Genome Res. *13*, 1810–1817. https://doi.org/10.1101/gr.1260903.

34. Xie, G., Johnson, S.L., Davenport, K.W., Rajavel, M., Waldminghaus, T., Detter, J.C., Chain, P.S., and Sozhamannan, S. (2017). Exception to the rule: genomic characterization of naturally occurring unusual vibrio cholerae strains with a single chromosome. Int. J. Genom. *2017*, 8724304. https://doi.org/10.1155/2017/8724304.

35. Val, M.E., Kennedy, S.P., Soler-Bistué, A.J., Barbe, V., Bouchier, C., Ducos-Galand, M., Skovgaard, O., and Mazel, D. (2014). Fuse or die: how to survive the loss of Dam in Vibrio cholerae. Mol. Microbiol. *91*, 665–678. https://doi.org/10.1111/mmi.12483.

36. Bruhn, M., Schindler, D., Kemter, F.S., Wiley, M.R., Chase, K., Koroleva, G.I., Palacios, G., Sozhamannan, S., and Waldminghaus, T. (2018). Functionality of two origins of replication in Vibrio cholerae strains with a single chromosome. Front. Microbiol. *9*, 2932. https://doi.org/10.3389/fmicb.2018.02932.

37. Mori, J.F., and Kanaly, R.A. (2022). Natural chromosome-chromid fusion across rRNA operons in a Burkholderiaceae bacterium. Microbiol. Spectr. *10*, e0222521. https://doi.org/10.1128/spectrum.02225-21.

38. Mavingui, P., Flores, M., Guo, X., Davila, G., Perret, X., Broughton, W.J., and Palacios, R. (2002). Dynamics of genome architecture in Rhizobium sp. strain NGR234. J. Bacteriol. *184*, 171–176. https://doi.org/10.1128/JB.184.1.171-176.2002.

39. diCenzo, G.C., and Finan, T.M. (2017). The divided bacterial genome: structure, function, and evolution. Microbiol. Mol. Biol. Rev. *81*, e00019-17. https://doi.org/10.1128/MMBR.00019-17.

40. Harrison, P.W., Lower, R.P., Kim, N.K., and Young, J.P.W. (2010). Introducing the bacterial 'chromid': not a chromosome, not a plasmid. Trends Microbiol. *18*, 141–148. https://doi.org/10.1016/j.tim.2009.12.010.

41. Wang, X., Llopis, P.M., and Rudner, D.Z. (2013). Organization and segregation of bacterial chromosomes. Nat. Rev. Genet. *14*, 191–203. https://doi.org/10.1038/nrg3375.

42. Deghelt, M., Mullier, C., Sternon, J.F., Francis, N., Laloux, G., Dotreppe, D., Van der Henst, C., Jacobs-Wagner, C., Letesson, J.J., and De Bolle, X. (2014). G1-arrested newborn cells are the predominant infectious form of the pathogen Brucella abortus. Nat. Commun. *5*, 4366. https://doi.org/10.1038/ncomms5366.

43. Rudner, D.Z., Fawcett, P., and Losick, R. (1999). A family of membrane-embedded metalloproteases involved in regulated proteolysis of membrane-associated transcription factors. Proc. Natl. Acad. Sci. USA *96*, 14765–14770. https://doi.org/10.1073/pnas.96.26.14765.

44. Imakaev, M., Fudenberg, G., McCord, R.P., Naumova, N., Goloborodko, A., Lajoie, B.R., Dekker, J., and Mirny, L.A. (2012). Iterative correction of Hi-C data reveals hallmarks of chromosome organization. Nat. Methods *9*, 999–1003. https://doi.org/10.1038/nmeth.2148.

45. Paintdakhi, A., Parry, B., Campos, M., Irnov, I., Elf, J., Surovtsev, I., and Jacobs-Wagner, C. (2016). Oufti: an integrated software package for high-accuracy, high-throughput quantitative microscopy analysis. Mol. Microbiol. *99*, 767–777. https://doi.org/10.1111/mmi.13264.

46. Morton, E.R., and Fuqua, C. (2012). Laboratory maintenance of Agrobacterium. Curr. Protoc. Microbiol. *Chapter 1*, Unit3D 1. https://doi.org/10.1002/9780471729259.mc03d01s24.

47. Wang, X., Le, T.B., Lajoie, B.R., Dekker, J., Laub, M.T., and Rudner, D.Z. (2015). Condensin promotes the juxtaposition of DNA flanking its loading site in Bacillus subtilis. Genes Dev. *29*, 1661–1675. https://doi.org/10.1101/gad.265876.115.

48. Ferrieres, L., Hemery, G., Nham, T., Guerout, A.M., Mazel, D., Beloin, C., and Ghigo, J.M. (2010). Silent mischief: bacteriophage Mu insertions contaminate products of Escherichia coli random mutagenesis performed using suicidal transposon delivery plasmids mobilized by broad-host-range RP4 conjugative machinery. J. Bacteriol. *192*, 6418–6427. https://doi.org/10.1128/JB.00621-10.

49. van Opijnen, T., Lazinski, D.W., and Camilli, A. (2014). Genome-wide fitness and genetic interactions determined by Tn-seq, a high-throughput massively parallel sequencing method for microorganisms. Curr. Protoc. Mol. Biol. *106*, 7.16.1–7.16.24. https://doi.org/10.1002/0471142727.mb0716s106.

50. Meeske, A.J., Sham, L.T., Kimsey, H., Koo, B.M., Gross, C.A., Bernhardt, T.G., and Rudner, D.Z. (2015). MurJ and a novel lipid II flippase are required for cell wall biogenesis in Bacillus subtilis. Proc. Natl. Acad. Sci. USA *112*, 6437–6442. https://doi.org/10.1073/pnas.1504967112.

51. Wang, X., and Montero Llopis, P. (2016). Visualizing Bacillus subtilis during vegetative growth and spore formation. Methods Mol. Biol. *1431*, 275–287. https://doi.org/10.1007/978-1-4939-3631-1_19.

52. Hinz, A.J., Larson, D.E., Smith, C.S., and Brun, Y.V. (2003). The Caulobacter crescentus polar organelle development protein PodJ is differentially localized and is required for polar targeting of the PleC development regulator. Mol. Microbiol. *47*, 929–941. https://doi.org/10.1046/j.1365-2958.2003.03349.x.

53. Fellay, R., Frey, J., and Krisch, H. (1987). Interposon mutagenesis of soil and water bacteria: a family of DNA fragments designed for in vitro insertional mutagenesis of gram-negative bacteria. Gene *52*, 147–154. https://doi.org/10.1016/0378-1119(87)90041-2.

54. Wang, X., Montero Llopis, P., and Rudner, D.Z. (2014). Bacillus subtilis chromosome organization oscillates between two distinct patterns. Proc. Natl. Acad. Sci. USA *111*, 12877–12882. https://doi.org/10.1073/pnas.1407461111.

55. Wang, X., Tang, O.W., Riley, E.P., and Rudner, D.Z. (2014). The SMC condensin complex is required for origin segregation in Bacillus subtilis. Curr. Biol. *24*, 287–292. https://doi.org/10.1016/j.cub.2013.11.050.

56. Madabhushi, R., and Marians, K.J. (2009). Actin homolog MreB affects chromosome segregation by regulating topoisomerase IV in Escherichia coli. Mol. Cell *33*, 171–180. https://doi.org/10.1016/j.molcel.2009.01.001.

57. Simon, R.P., Priefer, U., and Pühler, A. (1983). A broad host range mobilization system for in vivo genetic engineering: transposon mutagenesis in gram negative bacteria. Nat. Biotechnol. *1*, 784–791. https://doi.org/10.1038/nbt1183-784.

58. Barton, I.S., Platt, T.G., Rusch, D.B., and Fuqua, C. (2019). Destabilization of the tumor-inducing plasmid from an octopine-type Agrobacterium tumefaciens lineage drives a large deletion in the co-resident at megaplasmid. G3 (Bethesda) *9*, 3489–3500. https://doi.org/10.1534/g3.119.400554.

Please cite this article in press as: Liao et al., A dicentric bacterial chromosome requires XerC/D site-specific recombinases for resolution, Current Biology (2022), https://doi.org/10.1016/j.cub.2022.06.050

CellPress

STAR★METHODS

KEY RESOURCES TABLE

REAGENT or RESOURCE	SOURCE	IDENTIFIER
Antibodies		
Anti-GFP polyclonal rabbit antibody, affinity purified	[43]	N/A
Chemicals, peptides, and recombinant proteins		
Biotin-14-dATP	ThermoFisher	Cat # 19524016
Carbenicillin	GoldBio	Cat # C-103-5
Chloroform	VWR	Cat # MK444004
CIP	NEB	Cat # M0525L
Cumate	VWR	Cat # 103852-040
dCTP, dGTP, dTTP	Fisher	Cat # R0182
EDTA	VWR	Cat # EM-4050
Formaldehyde 37%	Sigma	Cat # F8775
Gentamicin	ACROS Organics	Cat # AC613980010
Glycine	VWR	Cat # JT4059-6
HindIII	NEB	Cat # R0104M
Isoamyl alcohol	VWR	Cat # JT9054-1
IPTG	Dot Scientific	Cat # DS102125
Kanamycin	IBI	Cat # IB02120
Klenow	NEB	Cat # M0210L
MmeI	NEB	Cat # R0637S
Proteinase K	NEB	Cat # P8107S
Phenol	VWR	Cat # 97064-822
Ready-Lyse Lysozyme	Epicenter	Cat # R1802M
RNase A	Promega	Cat # R7973
SDS	Calbiochem	Cat # 7910-500GM
T4 DNA Ligase	NEB	Cat # M0202M
T4 DNA Polymerase	NEB	Cat # M0203L
Theophylline	Sigma	Cat # T1633-100G
Critical commercial assays		
NEBNext Ultra II DNA Library Prep Kit	NEB	Cat # E7645
QIAGEN DNeasy blood & tissue kit	QIAGEN	Cat # 69504
Monarch DNA Gel Extraction Kit	NEB	Cat # T1020S
Deposited data		
Hi-C, ChIP-Seq, WGS data	This study	NCBI SRA: PRJNA824072; See Table S2
Unprocessed Microscopy Images	Mendeley Data	https://doi.org/10.17632/crv96srkp4.1
Experimental models: Organism/strains		
Agrobacterium tumefaciens strains, see Table S3	N/A	N/A
Oligonucleotides		
See Table S4	N/A	N/A
Recombinant DNA		
See Table S3	N/A	N/A
Software and algorithms		
Artemis	Sanger	https://www.sanger.ac.uk/tool/artemis/
CLC Genomics Workbench	QIAGEN	https://digitalinsights.qiagen.com/products-overview/discovery-insights-portfolio/analysis-and-visualization/qiagen-clc-genomics-workbench/

(*Continued on next page*)

Please cite this article in press as: Liao et al., A dicentric bacterial chromosome requires XerC/D site-specific recombinases for resolution, Current Biology (2022), https://doi.org/10.1016/j.cub.2022.06.050

Continued

REAGENT or RESOURCE	SOURCE	IDENTIFIER
GraphPad Prism 8	GraphPad Software	https://www.graphpad.com/
Hiclib	[44]	https://github.com/mirnylab/hiclib-legacy
MATLAB	Mathworks	https://www.mathworks.com/products.html?s_tid=gn_ps
MEME	N/A	http://meme-suite.org/
NIS-Elements AR	Nikon	https://www.microscope.healthcare.nikon.com/products/software/nis-elements/nis-elements-advanced-research
MetaMorph	Molecular Devices	https://www.moleculardevices.com/
Oufti	[45]	http://www.oufti.org/
R	N/A	https://www.r-project.org/
Other		
96-well microplate	Corning	Cat # 3603
Ampure Beads	Beckman	Cat # A63881
Glass-bottom dish	Willco Wells	Cat # HBSt-5040
ProteinA Magnetic Beads	GE Healthcare/cytiva	Cat # 28951378
Streptavidin Beads MyOne	Invitrogen	Cat # 65-001

RESOURCE AVAILABILITY

Lead contact

Further information and requests for resources and reagents should be directed to and will be fulfilled by the lead contact, Xindan Wang (xindan@indiana.edu).

Materials availability

Plasmids and strains generated in this study are available from the lead contact with a completed Materials Transfer Agreement.

Data and code availability

Unprocessed microscopy images are available at Mendeley data: https://doi.org/10.17632/crv96srkp4.1. Hi-C, ChIP-seq and WGS data were deposited to the NCBI Sequence Read Archive (accession no. PRJNA824072). This paper does not report original code. Any additional information required to analyze the data reported in this paper is available from the lead contact upon request without restriction.

EXPERIMENTAL MODEL AND SUBJECT DETAILS

Bacterial strains and growth

A. tumefaciens cells were grown in defined ATGN minimal medium[46] or LB broth as specified at 30°C with aeration. In liquid media, when appropriate, antibiotics or supplements were added at the following concentrations: kanamycin (IBI, IB02120) 150 μg/ml, carbenicillin (GoldBio, C-103-5) 25 μg/ml, gentamicin (ACROS Organics, AC613980010) 150 μg/ml, IPTG (Dot Scientific, DS102125) 0.25 or 0.5 mM, theophylline (Sigma, T1633-100G) 2 mM and cumate (VWR, 103852-040) 2 mM. Antibiotic concentrations were doubled when applied on solid media. Lists of Next-Generation-Sequencing samples, bacterial strains and plasmids, and oligonucleotides used in this study can be found in Tables S2, S3, and S4.

METHODS DETAILS

Hi-C

The Hi-C procedure was carried out as previously described.[6,47] Specifically, cells grown at the desired condition were crosslinked with 3% formaldehyde at room temperature for 30 min then quenched with 125 mM glycine. Cells were lysed using Ready-Lyse Lysozyme (Epicentre, R1802M) and treated by 0.5% SDS. Solubilized chromatin was digested with HindIII for 2 hours at 37°C. The digested ends were filled in with Klenow and Biotin-14-dATP, dGTP, dCTP, dTTP. The products were ligated with T4 DNA ligase at 16°C for about 20 hr. Crosslinks were reversed at 65°C for about 20 hr in the presence of EDTA, proteinase K and 0.5% SDS. The DNA was then extracted twice with phenol/chloroform/isoamylalcohol (25:24:1) (PCI), precipitated with ethanol, and resuspended in 20 μl of 0.1XTE buffer. Biotin from non-ligated ends was removed using T4 polymerase (4 hr at 20°C) followed by extraction with PCI. The DNA was then sheared by sonication for 12 min with 20% amplitude using a Qsonica Q800R2 water bath sonicator. The

Please cite this article in press as: Liao et al., A dicentric bacterial chromosome requires XerC/D site-specific recombinases for resolution, Current Biology (2022), https://doi.org/10.1016/j.cub.2022.06.050

sheared DNA was used for library preparation with the NEBNext UltraII kit (E7645). Biotinylated DNA fragments were purified using 10 μl streptavidin beads. DNA-bound beads were used for PCR in a 50 μl reaction for 14 cycles. PCR products were purified using Ampure beads (Beckman, A63881) and sequenced at the Indiana University Center for Genomics and Bioinformatics using NextSeq500. Paired-end sequencing reads were mapped to the combined genome files of *A. tumefaciens* C58 (NCBI Reference Sequence GCA_000092025.1). The genome was divided into 10-kb bins. Subsequent analysis and visualization were done using R. To put *ori1* at the center of Ch1, the reference genome of Ch1 starts at 1400 kb. The rearranged genome of the fusion strain was pieced together in the following order: Ch2 0.001 kb - 712.671 kb, Ch1 1793.369 kb - 2841.580 kb, Ch1 0.001 kb - 1793.368 kb, Ch2 712.672 kb -2075.577 kb, pAt 0.001 kb - 542.868 kb, pTi 0.001 kb - 214.233 kb. Note that the genome of the fusion strain had deletions of Ch1 1175.9 kb - 1186.195 kb and pAt 206.308 kb - 400.732 kb.

ChIP-seq

Chromatin immunoprecipitation (ChIP) for *A. tumefaciens* was performed as described previously.[47] Briefly, cells were crosslinked using 3% formaldehyde for 30 min at room temperature and then quenched using 125 mM glycine, washed using PBS, and lysed using lysozyme. Crosslinked chromatin was sheared to an average size of 250 bp by sonication using Qsonica Q800R2 water bath sonicator. The lysate was precleared using ProteinA magnetic beads (GE Healthcare/cytiva 28951378) and was then incubated with anti-GFP antibodies[43] overnight at 4°C. Next day, the lysate was incubated with ProteinA magnetic beads for 1h at 4°C. After washes and elution, the immunoprecipitate was incubated at 65°C overnight to reverse the crosslinks. The DNA was further treated with RNaseA, Proteinase K, extracted with PCI, resuspended in 100 μl EB and used for library preparation with the NEBNext UltraII kit (E7645). The library was sequenced using Illumina NextSeq500 at IU Center for Genomics and Bioinformatics. The sequencing reads were mapped to the combined *A. tumefaciens* C58 genome (NCBI GCA_000092025.1) using CLC Genomics Workbench (CLC Bio, QIAGEN). Sequencing reads from each ChIP and input sample were normalized by the total number of reads. The ChIP enrichment (ChIP/Input) was plotted and analyzed using R.

Identification of *dif* sites

In ChIP plots of XerC-GFP and XerD-GFP, three peaks with greater than 15-fold ChIP/Input enrichment were identified in all ChIP samples. By checking accurate locations of each peak using CLC Genomics Workbench (CLC Bio, QIAGEN), we excluded the one on pAt plasmid which was observed in every ChIP-seq experiment we have done on *A. tumefaciens* using anti-GFP antibodies regardless of strains used (Figure S2C, asterisk marked). The other two sites on Ch1 and pAt were seen in all XerC-GFP and XerD-GFP samples (Figure S2C). We used these two strong sites to search for the binding motif by MEME (http://meme-suite.org/) and identified a 26 bp consensus sequence which contains 23 consensus nucleotide positions and 3 degenerate positions (Figure S2D).

Whole genome sequencing (WGS)

Approximately $5x10^9$ exponentially growing cells were collected for each WGS. Genomic DNA was extracted using Qiagen DNeasy Kit (69504), sonicated using a Qsonica Q800R2 water bath sonicator, prepared using the NEBNext UltraII kit (E7645), and sequenced using Illumina NextSeq500. The reads were mapped to the *A. tumefaciens* C58 genome (NCBI GCA_000092025.1) using CLC Genomics Workbench (CLC Bio, QIAGEN). The mapped reads were normalized by the total number of reads. Relative copy numbers were calculated by dividing normalized reads with the averaged total number of reads at the terminus of Ch1 or at the left terminus of the fused chromosome. Plotting and analysis were performed using R.

Transposon insertion sequencing (Tn-seq)

To prepare transposon libraries, *Mariner* transposon-based plasmid (pTND2823, gift from Triana Dalia and Ankur Dalia at Indiana University) was transformed into an auxotrophic donor strain, *MFDpir E. coli*,[48] and then conjugated into *A. tumefaciens*. To generate a deep library, $1x10^6$ kanamycin-resistant conjugants were evenly plated on 10 large plates (150 mm diameter, VWR 25384-326) containing LB or ATGN with 300 μg/ml Kanamycin. The plates were incubated at 30°C for two days for LB or three days for ATGN. Colonies of the 10 plates from the same condition were scraped and combined into a single pool. 5 OD_{600} units of cells from the pool were used for genomic DNA (gDNA) isolation using QIAGEN DNeasy blood & tissue kit (69504). 3 μg of gDNA was digested with MmeI (NEB R0637S) for 90 min, and quick CIP (NEB M0525L) for 60 min at 37°C. The DNA was extracted using Phenol-Chloroform, precipitated using ethanol and resuspended in 15 μl ddH_2O. The digested end was ligated to an annealed adapter[49] using T4 DNA ligase and incubated at 16°C for about 16 hr. Adapter-ligated DNA was amplified with the primers complementary to the adapter and transposon inverted repeat sequence. The PCR product was gel purified using Monarch DNA Gel Extraction Kit (NEB T1020S) and sequenced at the IU Center for Genomics and Bioinformatics using NextSeq500. Sequencing reads were mapped to the combined genome files of *A. tumefaciens* C58 (NCBI Reference Sequence GCA_000092025.1) and analyzed using a procedure that was described before.[49,50] The results were visualized using Artemis (https://www.sanger.ac.uk/tool/artemis/).

Growth curve measurement

In Figure 2B, WT original strain (AtWX063) and WT fusion strain (AtWX001) were grown in LB or ATGN liquid medium overnight at 30°C with aeration. Overnight cultures were back-diluted to OD_{600} of 0.02 for LB cultures and 0.05 for ATGN cultures. 200 μl of each diluted culture was transferred into 96-well microplate with lid (Corning 3603). To monitor cell growth, the OD_{600} was recorded every 30 min for a total of 24 hr using a Synergy H1 multimode microplate reader at 30°C with shaking. For each medium per strain, three biological

Please cite this article in press as: Liao et al., A dicentric bacterial chromosome requires XerC/D site-specific recombinases for resolution, Current Biology (2022), https://doi.org/10.1016/j.cub.2022.06.050

replicates were set up by inoculating cells in three independent culture tubes. This experiment was performed twice on two different days and the results were combined. Plotting and analysis were performed using GraphPad Prism 8.

Fluorescence microscopy analysis

Fluorescence microscopy was performed on a Nikon Ti2E microscope equipped with Plan Apo 100x/1.4NA phase contrast oil objective and an sCMOS camera. Cells were immobilized using 2% agarose pads containing growth media. To determine cellular localization of origins, image analyses were performed using the MathWorks MATLAB-based program Oufti.[45] Cell outline and localizations of fluorescent foci were detected and plotted as described previously.[6]

In XerC/D depletion time-course experiments, cells were grown in LB medium containing inducers (0.5 mM IPTG and 2 mM theophylline) overnight. For XerC(+) and XerD(+) cells, subcultures were set up in 25 mL of LB medium containing inducers . Exponentially growing cells were collected for imaging. For XerC(-) and XerD(-) cells, inducers were washed off using LB medium for 3 times, and cells were sub-cultured in LB medium without inducers. At 3 hr, 6 hr, 12 hr, 18 hr post-subculturing, cells were collected for snapshot imaging. To prevent cells from entering stationary phase, when the OD_{600} reached 0.6, cultures were diluted to pre-warmed fresh medium.

In time-lapse imaging, for WT fusion strain having *dif1* labeled (AtWX455), cells were grown in LB medium overnight and then were sub-cultured in 25 ml of LB medium at initial OD_{600} of 0.04. For XerC(-) strains (AtWX467 and AtWX514), cells were grown in LB medium containing inducers (0.5 mM IPTG and 2 mM theophylline) overnight. Then inducers were washed off using LB medium for 3 times and then cells were sub-cultured in 25 ml of LB medium at initial OD_{600} of 0.04. After 6-hour depletion, cells were collected for time-lapse imaging. A glass bottom dish (Willco dish HBSt-5040; Willco Wells) was used as a coverslip.[51] Cells were concentrated and spotted onto the glass bottom dish. A 2% LB agarose strip was then laid on top of the cells. The agarose strip was fully exposed to adequate oxygen for cell growth. The dish was placed in a temperature-controlled incubator.[51] Cells were imaged every 10 min. Images were processed using MetaMorph software (Molecular Devices).

Plasmid construction

pWX811 [pNPTS138 *ΔrepB*^{Ch2} (Atu3923/ATU_RS18280) (*kan*)] was constructed by an isothermal assembly reaction containing three gel-purified fragments: 1) pNPTS138 digested by EcoRV; 2) *repB*^{Ch2} upstream region amplified using oWX2021 and oWX2022 from C58 gDNA; 3) *repB*^{Ch2} downstream region amplified using oWX2023 and oWX2024 from C58 gDNA. The construct was sequenced using oWX1854 and oWX1855.

pWX813 [pMiniTn7 *pLac repB*^{Ch2} (Atu3923/ATU_RS18280) *kan* (*gen*)] was constructed by a ligation reaction containing two DNA fragments: 1) pUC18-mini-Tn7T-GM-Plac-HA[9] digested by NdeI and XhoI; 2) *repB*^{Ch2} amplified using oWX2027 and oWX2028 from C58 gDNA. The construct was sequenced using oWX2031 and oWX2042.

pWX855 [pNPTS138 Δ*xerD* (Atu3629/ATU_RS16850)::*amp* (*kan*)] was constructed by an isothermal assembly reaction containing four gel-purified fragments: 1) EcoRV-digested pNPTS138;[52] 2) *At xerD* (Atu3629/ATU_RS16850) upstream region amplified using oWX2144 and oWX2208 from C58 genomic DNA; 3) *At xerD* (Atu3629/ATU_RS16850 downstream region amplified using oWX2146 and oWX2209 from C58 genomic DNA; 4) *amp* amplified using oWX2210 and oWX2211 from plasmid pHP45omega.[53] The construct was sequenced using oWX1854 and oWX1855.

pWX923 [pACYC *terminator Ppen cfp-parB*^{P1}*-parS*^{P1} *terminators amp*] was constructed by an isothermal assembly reaction containing two gel-purified fragments: 1) SalI/EagI-digested pWX916;[7] 2) terminators amplified using oWX2403 and oWX2404 from genomic DNA of BWX925.[54] The construct was sequenced using oWX2395.

pWX926 [pNPTS138 *Ppen ygfp-parB*^{MT1}*-parS*^{MT1} at Atu1460/ATU_RS07195 (*kan*)] was constructed by an isothermal assembly reaction containing four gel-purified fragments: 1) EcoRV-digested pNPTS138;[52] 2) a part of Atu1460/ATU_ RS07195 amplified using oWX2409 and oWX2410 from C58 gDNA; 3) *ygfp-parB*^{MT1}*-parS*^{MT1} amplified using oWX2407 and oWX2408 from pWX924;[6] 4) a part of Atu1461/ATU_ RS07195 amplified using oWX2411 and oWX2412 from C58 gDNA. The construct was sequenced using oWX2379, oWX2418, oWX2419 and oWX2426.

pWX943 [pNPTS138 *terminator gen lacI terminators Plac-riboswitch* (*kan*)] was constructed by an isothermal assembly reaction containing three gel-purified fragments: 1) EcoRV-digested pNPTS138;[52] 2) *terminator gen lacI terminators Plac* was generated using oWX2482 and oWX2450 on pUC18-mini-Tn7T-GM-Plac-HA;[9] 3) Riboswitch was amplified using oWX2451 and oWX2452 from pJZ274.[15] The construct was sequenced oWX1854, oWX1855, oWX2491, oWX2492 and oWX2493.

pWX944 [pNPTS138 *terminator gen lacI terminators Plac-riboswitch* inserted before *xerC* (Atu2628/ATU_RS12790) (*kan*)] was constructed by an isothermal assembly reaction containing four gel-purified fragments: 1) EcoRV-digested pNPT138;[52] 2) *At xerC* (Atu2628/ATU_RS12790) upstream region amplified using oWX2453 and oWX2483 from C58 genomic DNA; 3) *gen lacI-Plac-riboswitch* amplified using oWX2484 and oWX2456 from plasmid pWX943; 4) A part of *At xerC* (Atu2628/ATU_RS12790) amplified using oWX2457 and oWX2458 from C58 genomic DNA. The construct was sequenced using oWX1854 and oWX1855.

pWX945 [pNPTS138 *terminator gen lacI terminators Plac-riboswitch* inserted before *xerD* (Atu3629/ATU_RS16850) (*kan*)] was constructed by an isothermal assembly reaction containing four gel-purified fragments: 1) EcoRV-digested pNPT138;[52] 2) *At xerD* (Atu3629/ATU_RS16850) upstream region amplified using oWX2459 and oWX2485 from C58 genomic DNA; 3) *gen lacI-Plac-riboswitch* amplified using oWX2486 and oWX2462 from plasmid pWX943; 4) A part of *At xerD* (Atu3629/ATU_RS16850) amplified using oWX2463 and oWX2464 from C58 genomic DNA. The construct was sequenced using oWX1854 and oWX1855.

pWX965 [pNPTS138 *PT7strong ygfp-parB^{MT1}-parS^{MT1}* at Atu1460/ATU_RS07195] was constructed by an isothermal assembly reaction containing one gel-purified fragments: pWX926 backbone amplified using oWX2431 and oWX2432. The construct was sequenced using oWX2379, oWX2418, oWX2419 and oWX2426.

pWX968 [pNPTS138 *PT7strong cfp-parB^{P1}-parS^{P1}* at Atu4854 (*kan*)] was constructed by an isothermal assembly reaction containing four gel-purified fragments: 1) EcoRV-digested pNPTS138;[52] 2) *PT7strong cfp-parB^{P1}-parS^{P1}* amplified using oWX2407 and oWX2408 from pWX936;[7] 3) a part of Atu4854 amplified using oWX2514 and oWX2515 from C58 gDNA; 4) a part of Atu4855/ATU_22800 amplified using oWX2516 and oWX2517 from C58 gDNA. The construct was sequenced using oWX2377, oWX2426, oWX2518 and oWX2519.

pWX998 [pNPTS138 *PT7strong mcherry-parB^{P1}-parS^{P1}* at Atu4854 (*kan*)] was constructed by an isothermal assembly reaction containing two gel-purified fragments: 1) pWX968 backbone amplified using oWX2589 and oWX2590 on pWX968; 2) *mcherry* amplified using oWX2584 and oWX2585 from gDNA of BWX2208.[55] The construct was sequenced using oWX2377, oWX2426, oWX2518 and oWX2519.

pWX1006 [pNPTS138 Δ*xerC* (Atu2628/ATU_RS12790)::*amp* (*kan*)] was constructed by an isothermal assembly reaction containing four gel-purified fragments: 1) EcoRV-digested pNPTS138;[52] 2) *At xerC* (Atu2628/ATU_RS12790) upstream region amplified using oWX2601 and oWX2602 from C58 genomic DNA; 3) *At xerC* (Atu2628/ATU_RS12790) downstream region amplified using oWX2603 and oWX2604 from C58 genomic DNA; 4) *amp* amplified using oWX2210 and oWX2211 from plasmid pHP45omega.[53] The construct was sequenced using oWX2210, oWX2624 and oWX2625.

pWX1007 [pNPTS138 Δ*recA* (Atu1873/ATU_RS09160)::*amp* (*kan*)] was constructed by an isothermal assembly reaction containing four gel-purified fragments: 1) EcoRV-digested pNPTS138;[52] 2) *At recA* (Atu1873/ATU_RS09160) upstream region amplified using oWX2605 and oWX2606 from C58 genomic DNA; 3) *At recA* (Atu1873/ATU_RS09160) downstream region amplified using oWX2607 and oWX2608 from C58 genomic DNA; 4) *amp* amplified using oWX2210 and oWX2211 from plasmid pHP45omega.[53] The construct was sequenced using oWX2210, oWX2624 and oWX2625.

pWX1008 [pNPTS138 *xerC-gfpmut3* (Atu2628/ATU_RS12790) (*kan*)] was constructed by an isothermal assembly reaction containing four gel-purified fragments: 1) EcoRV-digested pNPTS138;[52] 2) a part of C terminal region of *At xerC* (Atu2628/ATU_RS12790) amplified using oWX2609 and oWX2610 from C58 genomic DNA; 3) *At xerC* (Atu2628/ATU_RS12790) downstream region amplified using oWX2613 and oWX2614 from C58 genomic DNA; 4) *gfpmut3* amplified using oWX2611 and oWX2612 on BWX2030.[47] The construct was sequenced using oWX2497, oWX2626, oWX2627 and oWX2628.

pWX1009 [pNPTS138 *xerD-gfpmut3* (Atu3629/ATU_RS16850) (*kan*)] was constructed by an isothermal assembly reaction containing four gel-purified fragments: 1) EcoRV-digested pNPTS138;[52] 2) a part of C terminal region of *At xerD* (Atu3629/ATU_RS16850) amplified using oWX2615 and oWX2616 from C58 genomic DNA; 3) *At xerD* (Atu3629/ATU_RS16850) downstream region amplified using oWX2617 and oWX2618 from C58 genomic DNA; 4) *gfpmut3* amplified using oWX2611 and oWX2612 on BWX2030.[47] The construct was sequenced using oWX2497, oWX2626, oWX2627 and oWX2628.

pWX1039 [pNPTS138 Δ*dif1*::*amp* (*kan*)] was constructed by an isothermal assembly reaction containing four gel-purified fragments: 1) EcoRV-digested pNPTS138;[52] 2) *dif1* upstream region amplified using oWX2796 and oWX2797 from C58 genomic DNA; 3) *dif1* downstream region amplified using oWX2800 and oWX2801 from C58 genomic DNA; 4) *amp* amplified using oWX2798 and oWX2799 from plasmid pHP45omega.[53] The construct was sequenced using oWX2210, oWX2624 and oWX2625.

pWX1040 [pNPTS138 Δ*dif^{pAt}*::*amp* (*kan*)] was constructed by an isothermal assembly reaction containing four gel-purified fragments: 1) EcoRV-digested pNPTS138;[52] 2) *dif^{pAt}* upstream region amplified using oWX2802 and oWX2803 from C58 genomic DNA; 3) *dif^{pAt}* downstream region amplified using oWX2806 and oWX2807 from C58 genomic DNA; 4) *amp* amplified using oWX2804 and oWX2805 from plasmid pHP45omega.[53] The construct was sequenced using oWX2210, oWX2624 and oWX2625.

pWX1076 [pSRKKm *cymR cuO Plac cuO At parC* (Atu1158/ATU_RS05720) *At parE* (Atu1622/ATU_RS07965) (*kan*)] was constructed by an isothermal assembly reaction containing three gel-purified fragments: 1) NdeI/NheI-digested plasmid pSRKKm *cuO Plac cuO msfgfp* (gift from Pam Brown); 2) *At parC* (Atu1158/ATU_RS05720) amplified using oWX2912 and oWX2913 from C58 genomic DNA; 3) optimized ribosomal binding site plus *At parE* (Atu1622/ATU_RS07965) amplified using oWX2914 and oWX2915 from C58 genomic DNA. The construct was sequenced using oWX2720, oWX2920, oWX2922, oWX2923, oWX2924, oWX2925, oWX2926 and oWX2927. Based on protein sequence alignment and gene synteny analysis, we note that *At parE* (Atu1622/ATU_RS07965) was mis-annotated as *gyrB* in NCBI Reference Sequence GCA_000092025.1*;* the bona fide *gyrB* is (Atu0012/ATU_RS00060).

pWX1080 [pSRKKm *cymR cuO Plac cuO Ec parE-parC* (*kan*)] was constructed by an isothermal assembly reaction containing two gel-purified fragments: 1) NdeI/NheI-digested plasmid pSRKKm *cuO Plac cuO msfgfp* (gift from Pam Brown); 2) *E.coli parE-parC* amplified using oWX2936 and oWX2939 on pLEXRparEC3.[56] The construct was sequenced using oWX2720, oWX2922, oWX2940, oWX2941, oWX2942, oWX2943, oWX2944 and oWX2945.

Strain construction

In general, in-frame deletions of C58 *A. tumefaciens* strains were constructed using a previously described allelic replacement method.[46] Briefly, regions flanking the gene to be deleted were PCR amplified using Q5 polymerase (NEB M0491) and cloned into pNPTS138,[52] a ColE1 suicide plasmid that confers kanamycin resistance and sucrose sensitivity, by isothermal assembly reactions. See Plasmid construction section for details. The pNPTS138 deletion plasmids were then introduced into *A. tumefaciens* C58 via mating with *E. coli* S17-1/λpir[57] carrying the appropriate construct. Screening for plasmid integration and target gene deletion was

Please cite this article in press as: Liao et al., A dicentric bacterial chromosome requires XerC/D site-specific recombinases for resolution, Current Biology (2022), https://doi.org/10.1016/j.cub.2022.06.050

performed as previously described.[46,58] The deletion mutants were confirmed by colony PCR. Specific information about each strain can be found below.

Fusion strain, *ori1* and *ori2* visualized by EGFP-ParB1 and RFP-RepB^{Ch2} (**AtWX366**) was generated by directly electroporating pWX970 into WT fusion strain (AtWX001).

Fusion strain, *tetRA::a-attTn7 pLac repB^{ch2} gen*, Δ*repB^{Ch2}* (**AtWX025**) was constructed in two steps: 1) *pLac repB^{ch2} gen* was inserted at the engineered a-attTn7 site using pWX813 in AtWX003[9] as pervious described;[9] 2) pWX811 was used to delete the endogenous *repB^{Ch2}* in presence of 0.5 mM IPTG. The deletion was confirmed oWX2021 and oWX2024.

Fusion strain, *terminator gen lacI terminators Plac-riboswitch-xerC* (**AtWX323**) was generated using pWX944 to introduce *terminator gen LacI terminators Plac-riboswitch* before start codon of *xerC* (Atu2628/ATU_RS12790) in the fusion strain (AtWX001) and confirmed using oWX487 and oWX2029.

Fusion strain, *terminator gen lacI terminators Plac-riboswitch-xerD* (**AtWX327**) was generated using pWX945 to introduce *terminator gen LacI terminators Plac-riboswitch* before start codon of *xerD* (Atu3629/ATU_RS16850) in the fusion strain (AtWX001) and confirmed using oWX487 and oWX2029.

Original strain, *terminator gen lacI terminators Plac-riboswitch-xerC* (**AtWX331**) was generated using pWX944 to introduce *terminator gen LacI terminators Plac-riboswitch* before start codon of *xerC* (Atu2628/ATU_RS12790) in the original strain (AtWX063) and confirmed using oWX487 and oWX2029.

Original strain, *terminator gen lacI terminators Plac-riboswitch-xerD* (**AtWX332**) was generated using pWX945 to introduce *terminator gen LacI terminators Plac-riboswitch* before start codon of *xerD* (Atu3629/ATU_RS16850) in the original strain (AtWX063) and confirmed using oWX487 and oWX2029.

ΔrecA fusion strain (**AtWX387**) was generated by conjugating pWX1007 into the fusion strain (AtWX001) and confirmed using oWX2210, 2624, 2625.

ΔrecA original strain (**AtWX398**) was generated by conjugating pWX1007 into the original strain (AtWX063) and confirmed using oWX2210, 2624, 2625.

Δsmc fusion strain (**AtWX035**) was generated by conjugating pWX832 into the fusion strain (AtWX001) and confirmed using oWX2085 and oWX2086.

Fusion strain, *yGFP-parB^{MT1}-parS^{MT1}* inserted between Atu1460/ATU_RS07195 and Atu1461/ ATU_RS07200 22 kb from *dif1* (**AtWX455**) was generated by conjugating pWX965 into WT fusion strain (AtWX001) and confirmed using oWX2418 and oWX2419.

Fusion strain with XerC depletion, *yGFP-parB^{MT1}-parS^{MT1}* inserted between Atu1460/ATU_RS07195 and Atu1461/ ATU_RS07200 22 kb from *dif1* **(AtWX467**) was generated by conjugating pWX965 into XerC depletion strain (AtWX323) and confirmed using oWX2418 and oWX2419.

Fusion strain with XerD depletion, *yGFP-parB^{MT1}-parS^{MT1}* inserted between Atu1460/ATU_RS07195 and Atu1461/ ATU_RS07200 22 kb from *dif1* (**AtWX471**) was generated by conjugating pWX965 into XerD depletion strain (AtWX327) and confirmed using oWX2418 and oWX2419.

Original strain, *xerC-gfpmut3* (**AtWX377**) was generated by conjugating pWX1008 into the original strain (AtWX063) and confirmed using oWX2497 and oWX2627.

Original strain, *xerD-gfpmut3* (**AtWX370**) was generated by conjugating pWX1009 into the original strain (AtWX063) and confirmed using oWX2497 and oWX2627.

Fusion strain, *xerC-gfpmut3* (**AtWX367**) was generated by conjugating pWX1008 into the fusion strain (AtWX001) and confirmed using oWX2497 and oWX2627.

Fusion strain, *xerD-gfpmut3* (**AtWX379**) was generated by conjugating pWX1009 into the fusion strain (AtWX001) and confirmed using oWX2497 and oWX2627.

ΔxerD original strain (**AtWX092**) was generated by conjugating pWX855 into the original strain (AtWX063) and confirmed using oWX2148 and oWX2149.

ΔxerC original strain (**AtWX375**) was generated by conjugating pWX1006 into the original strain (AtWX063) and confirmed using oWX2210, 2624, 2625.

Δdif1 original strain (**AtWX439**) was generated by conjugating pWX1039 into the original strain (AtWX063) and confirmed using oWX2847 and oWX2848.

Δdif^{pAt} fusion strain (**AtWX440**) was generated by conjugating pWX1040 into the fusion strain (AtWX001) and confirmed using oWX2849 and oWX2850.

Δdif^{pAt} original strain (**AtWX441**) was generated by conjugating pWX1040 into the original strain (AtWX063) and confirmed using oWX2849 and oWX2850.

Fusion strain with XerC depletion, *yGFP-parB^{MT1}-parS^{MT1}* inserted between Atu1460/ATU_RS07195 and Atu1461/ ATU_RS07200 22 kb from *dif1, mcherry-parB^{P1}-parS^{P1} inserted between Atu4854 and Atu4855, 39.8 kb from right ter* (**AtWX514**) was generated by conjugating pWX998 into AtWX467 and confirmed using oWX2518 and oWX2519.

For strains containing plasmids for overexpressing *A. tumefaciens* Topo IV or *E. coli* Topo IV, pWX1076 or pWX1080 was directly electroporated into fusion strains with XerC depletion (AtWX323) or XerD depletion (AtWX327) as previously described[46] to generate **AtWX502**, **AtWX503**, **AtWX540, and AtWX541**.

Please cite this article in press as: Liao et al., A dicentric bacterial chromosome requires XerC/D site-specific recombinases for resolution, Current Biology (2022), https://doi.org/10.1016/j.cub.2022.06.050

QUANTIFICATION AND STATISTICAL ANALYSIS

Localization of *ori1* and *ori2*

To quantify distribution and colocalization of fluorescence foci, we analyzed images using the MathWorks MATLAB-based program Oufti[45] as described previously.[6] Briefly, cell outlines were detected using the cellDetection module. Localizations of fluorescent foci were identified using the spotDetection module. Subsequently, manual inspection was employed to remove the cell meshes with wrongly detected cell outlines or spots. The data were further analyzed and plotted in MATLAB. In our snapshot images, the average diameter of a fluorescence focus was 6 pixels. As such, the spatial relationship of foci was defined as colocalizing when red and green foci had inter-focal distance of less than 6 pixels.

Measurements of doubling time and growth curve

Measurements were performed in biological triplicates. Two independent growth curve measurements were carried out. Plotting and analysis were performed using GraphPad Prism 8. Data were presented as the Means ± Standard Deviations (SDs).

Quantitative analysis of *dif1* localization patterns

To quantitatively analyze *dif1* localization pattern, we analyzed snapshot images from time-course experiments using NIS-Elements software. Cells were classified in terms of cell cycle and foci number. 700∼1200 cells were analyzed for each sample and counted manually using counter mode in NIS-Elements AR.